



Fragment-based discovery of JAK-2 inhibitors

Stephen Antonyssamy, Gavin Hirst*, Frances Park, Paul Sprengeler, Frank Stappenbeck, Ruo Steensma, Mark Wilson, Melissa Wong

Medicinal Chemistry, SGX Pharmaceuticals, Inc., 10505 Roselle Street, San Diego, CA 92121, USA

ARTICLE INFO

Article history:

Received 7 July 2008

Revised 18 August 2008

Accepted 18 August 2008

Available online 22 August 2008

Keywords:

Fragment-based design

JAK-2 inhibitors

Structure-based design

Aminoindazole

Kinase inhibitors

ABSTRACT

Fragment-based hit identification coupled with crystallographically enabled structure-based drug design was used to design potent inhibitors of JAK-2. After two iterations from fragment **1**, we were able to increase potency by greater than 500-fold to provide sulfonamide **13**, a 78-nM JAK-2 inhibitor.

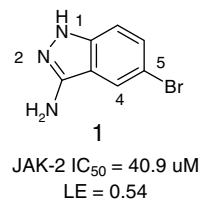
© 2008 Published by Elsevier Ltd.

The Janus Kinase (JAK) family comprises four cytoplasmic receptor-associated protein tyrosine kinases, JAK-1, JAK-2, JAK-3, and Tyk-2. Members of this enzyme family participate in signal transduction pathways mediated by many cytokines and cytokine-like hormones.¹ Initial biochemical studies implicated JAK-2 in the response to receptors from the single-chain and IL-3 cytokine families as well as the IFN- γ receptor.² Consistent with a critical role in erythropoiesis, knock-out of JAK-2 in mice is embryonically lethal.³ It is noteworthy that humans with JAK-2 mutations exhibit myeloproliferative disorders (MPD).⁴ Specifically, a characteristic somatic mutation, JAK-2 V617F, has recently been identified in patients with polycythemia vera, essential thrombocytosis, and myelofibrosis.⁵ This mutation results in a constitutively active JAK-2 tyrosine kinase. This gain-of-function mutation has stimulated discovery and development of inhibitors that selectively target JAK-2 as an approach toward directed therapy of MPD.⁶ This paper describes the identification of a series of potent JAK-2 wild-type (WT) and JAK-2 V617F inhibitors derived from a fragment-based approach.

Fragment-based lead discovery has been recently reviewed.⁷ In summary, the high screening hit rate for such small, low-MW compounds can often lead to the identification of novel, tractable hits and is recognized as a tangible alternative to more traditional high-throughput screening methods of hit identification. These highly ligand efficient (LE) starting points can be optimized into potent leads with good 'drug-like' properties. In particular, crystal-

lographic fragment screening can identify hits with low or undetectable potency in biochemical assays. Crystallographic fragment screening also provides unambiguous proof of binding to the target site and reveals the details of the hit's binding mode. This information provides clear direction for how they may be optimized into more potent lead compounds using efficient fragment elaboration.

We developed experimental protocols for growing JAK-2 crystals that were suitable for determining inhibitor co-crystal structures by soaking. Fragments in the SGX core screening library were chosen to be consistent with 'lead-like' properties, and also to include two or more substituents to facilitate rapid analog synthesis. The fragment library had a MW range of 100–220 Da and an average MW of 160.



Examination of a number fragments bound to JAK-2 revealed the bromoaminoindazole **1**, a 41- μ M JAK-2 inhibitor, as an attractive starting point, particularly given its high ligand efficiency. It is noteworthy that the corresponding 6-bromo analog is a less potent inhibitor (131 μ M). Analysis of the X-ray crystal structure of **1** bound to JAK-2 in Figure 1 revealed three hydrogen bonds between the aminoindazole and the hinge region. Specifically, the 3-amino

* Corresponding author. Tel.: +1 858 228 1630; fax: +1 858 588 0642.

E-mail address: hirst_gavin@lilly.com (G. Hirst).

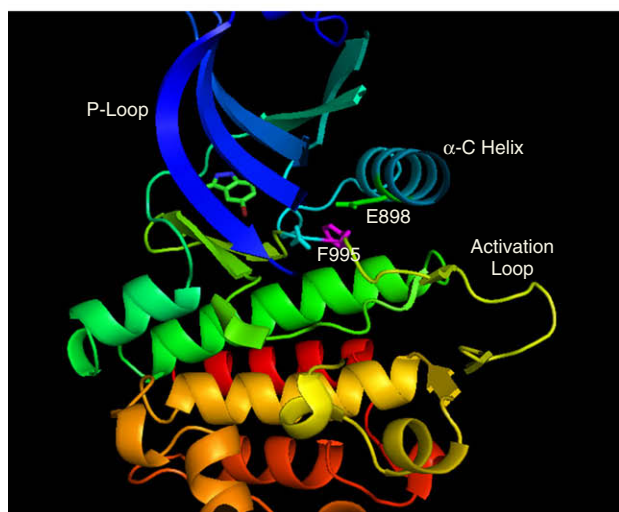
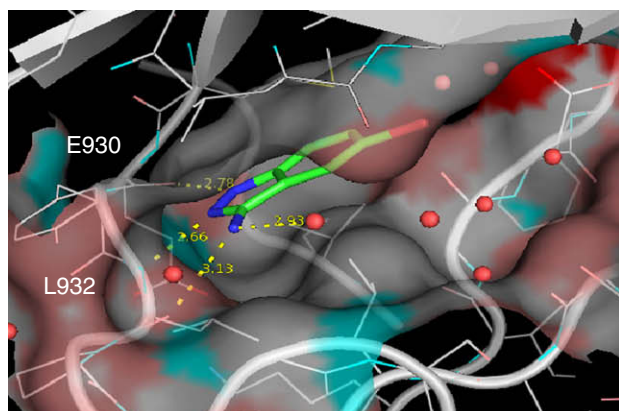


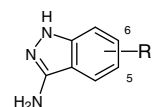
Figure 1. Crystal structure of **1** bound to JAK-2 at 1.9 Å resolution. PDB code 3E62.

bridges to the backbone carbonyl of Leu 932, the indazole 2-nitrogen to the NH of the same residue, and the 1-amino group to the carbonyl of Glu 930. The ligand is surrounded by lipophilic residues, in particular C-7 lies within 3.8 Å of the side chain of the gatekeeper methionine 929 at the rear of the pocket. Additionally, the top face of the indazole closest to the N-lobe of the catalytic domain interacts with the p-loop (the glycine-rich loop), Leu855, and Val863, which provide a lipophilic environment. Analogous interactions occur between Leu983 in the C-lobe and the opposite face of the planar ligand.

The bottom panel of Figure 1 shows that the catalytic domain of JAK-2 adopts an active conformation with both the α -C-Glu (E898 in green) and the conserved DFG 'in' (F995 in magenta) with the activation loop in an extended conformation.⁸ We elected to take advantage of a groove generated by the p-loop on the upper face and the start of the activation loop on the lower face. This trajectory could be achieved by modifications at C-5 and C-6 of the indazole although our initial analysis suggested that C-5 extensions would be the most desirable (Table 1).

Comparison of the two regioisomeric phenyl-substituted indazoles **2** and **3** was particularly instructive and supported our focus on the 5-position. The 5-phenyl analog **2** exhibited a 25-fold potency increase (LE = 0.49) compared to **1**, whereas the 6-phenyl analog **3** lost greater than 3-fold resulting in a 90-fold differentiation between the two compounds. As evident from the co-crystal structure of **2** bound to JAK-2 (Fig. 2), the 5-phenyl group is readily accommodated by both the p-loop and the aforementioned Val863.

Table 1
JAK-2 inhibition of 5- and 6-substituted aminoindazoles.



Compound	R ¹	JAK-2 IC ₅₀ (μM)	Ligand efficiency (kcal mol ⁻¹)
2	5-Ph	1.6	0.49
3	6-Ph	145.3	0.32
4	5-(3-Pyrazolyl)	9.3	0.45
5	5-(4-Pyridyl)	1.95	0.48
6	5-[4-(3,5-Dimethyl)isoxazolyl]	28.6	0.36
7	5-[5-(2,4-dimethyl)thiazolyl]	0.32	0.51
8	5-(2-Chlorophenyl)	0.37	0.52
9	5-(3-Chlorophenyl)	0.74	0.49
10	5-[6-Chloro-(2-pyridyl)]	5.8	0.41

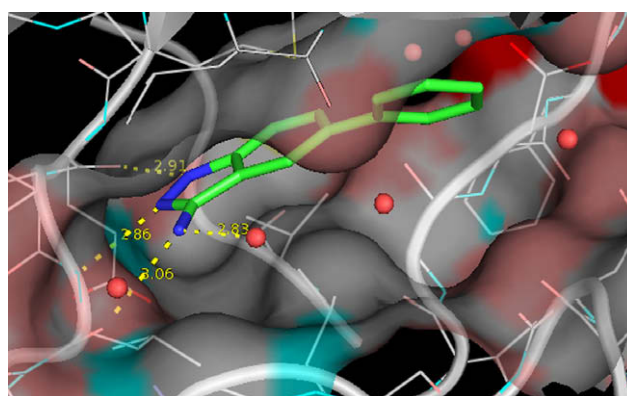


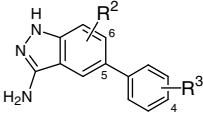
Figure 2. Crystal structure of **2** bound to JAK-2 at 1.8 Å resolution. PDB code 3E63.

Conversely, the IC₅₀ for indazole **3** is consistent with the fact that the C-6 substituent is oriented towards the polar residues of the catalytic Lys882 and also Glu994 of the DFG motif. By analogy with **2**, the potency of the 4-pyridyl analog **5** can be explained.

Substitution at either the 2- or 3-position on the 5-phenyl provides a modest potency increase, as seen for the chlorides **8** and **9**. The 8-fold potency loss between the 3-chlorophenyl analog **9** and the analogous 2-pyridyl indazole **10** suggests that polar groups are not tolerated at this position, a finding that is supported by pyrazole **4**. This election was guided by a number of aspects. First, compound **2** is a highly ligand efficient starting point (0.49 kcal mol⁻¹) a facet that represented a key driver to maintain drug-like properties during our lead optimization process. Second, further elaborations were readily accessed from available starting materials which allowed for a rapid SAR exploration. Conversely, other potential starting points with similar ligand efficiency such as the thiazole **7** were not pursued due to poor synthetic accessibility of analogs. We were particularly interested in identifying groups with additional productive Van der Waals (VdW) interactions within the p-loop. Inspection of our crystal structures suggested that this goal could be achieved from either the 3- or 4-position of the phenyl group (Table 2). The 4-*tert*-butyl sulfonamide **13** distinguished from the other analogs in Table 2, by inhibiting JAK-2 with an IC₅₀ of 78 nM while maintaining a high LE (0.41). All other compounds in Table 2 have lower ligand efficiencies than sulfonamide **13** (data not shown).

Figure 3 shows the crystal structure of **13** bound to JAK-2 with the *t*-butyl group nestled against the glycine-rich portion of the

Table 2
JAK-2 inhibition of 5-aryl substituted aminoindazoles.



Compound	R ³	R ²	JAK-2 IC ₅₀ (μM)
11	4(<i>N</i> -Me-piperazinyl)	H	8.58
12	3-SO ₂ NHtBu	H	3.55
13	4-SO ₂ NHtBu	H	0.078
14	4-CONHtBu	H	1.95
15	4-NHCONHtBu	H	3.9
16	4-CO-morpholino	H	1.57
17	4-CH ₂ -morpholino	H	1.11
18	4-SO ₂ Ethyl	H	0.79
19	4-SO ₂ -morpholino	H	0.33
20	4-SO ₂ NHtBu	7-Cl	1.22
21	4-SO ₂ NHtBu	7-Me	0.77
22	4-SO ₂ NHtBu; 2-Cl	H	0.039

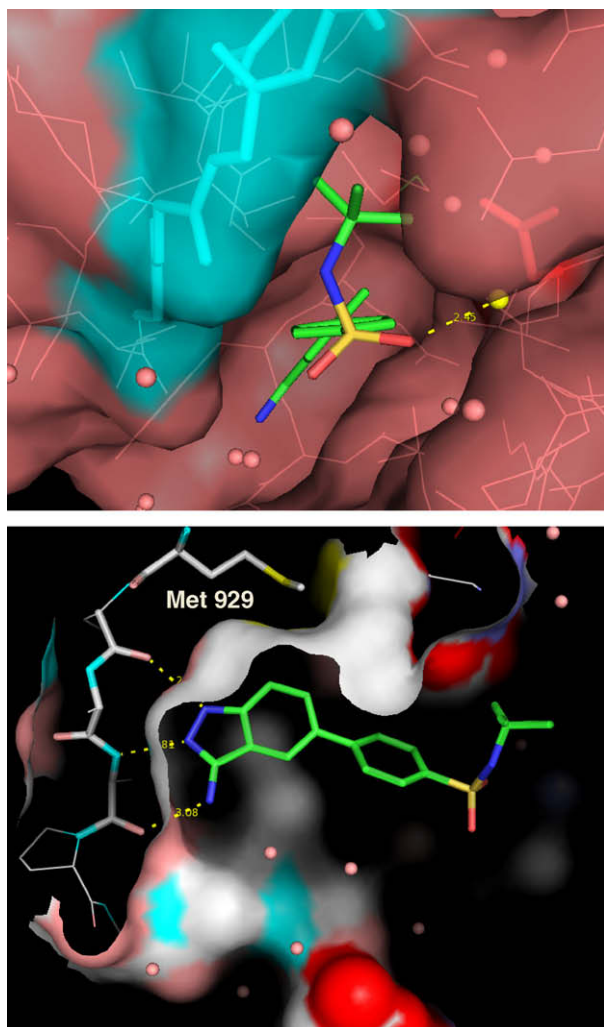


Figure 3. Crystal structure of **13** bound to JAK-2 at 1.7 Å resolution. PDB code 3E64.

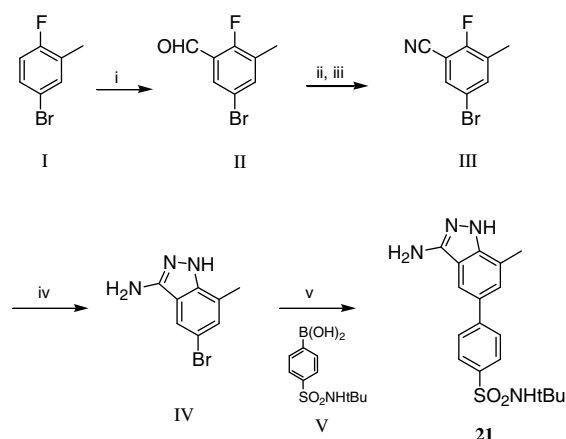
p-loop (shown in cyan in Fig. 3, top) and pointing towards the α-C-helix (not shown). The sulfonamide oxygen makes a water-bridged hydrogen bond to Asn981 in the C-lobe. Other data in Table 2 support the unique role of the sulfonamide group. In accord with precedent for aryl sulfonamides,⁹ both the nitrogen lone pair and the

carbon aromatic p-orbital bisect the O=S=O angle resulting in a conformation that places the aryl-sulfonyl torsion angle at 90°. This minimum energy conformation is not readily accessible to the amide **14** or the urea **15**, both of which have a preference for a planar conformation and is consistent with the lower potency of these analogs. The results of probing substitution at the 3-position (R₃) can be illustrated with a single example, as all similarly substituted analogs exhibited a reduction in potency compared to the corresponding 4-position congeners. Specifically, we observed a 45-fold reduction in potency for the 3-sulfonamide, compound **12**, compared to the 4-substituted sulfonamide **13**. It is of additional note that a similar optimization approach starting from the 5-(2-chlorophenyl) aminoindazole **8** resulted in the analogous 4-*tert*-butyl sulfonamide **22**, a more potent compound but with slightly lower ligand efficiency (0.39 kcal mol^{−1}) than its parent **13**.

The well-documented mobility of kinase catalytic domains suggested that we could further augment the potency of sulfonamide **13** by probing the region proximal to the lipophilic methionine 929 gatekeeper. Substitutions at the aminoindazole 7-position resulted in significant reductions in potency (7-chloro **20**: 15-fold; 7-methyl **21**: 10-fold), suggesting that the gatekeeper methionine is unable to move sufficiently to allow these groups to participate in productive VdW interactions.

The potency of these inhibitors for the V617F JAK-2 mutant and selectivity against JAK-3 was of particular interest in our ongoing design activities and proof-of-concept efforts. Accordingly, sulfonamide **13** was further profiled against these kinases and found to be a potent V617F JAK-2 inhibitor (IC₅₀ = 206 nM) with greater than 35-fold selectivity versus JAK-3 (IC₅₀ = 2.93 μM).

The aminoindazoles in this paper were prepared using the general synthetic methods shown in Scheme 1 and is illustrated for the synthesis of target molecule **21**. *ortho*-Lithiation of the fluorotoluene **I** followed by quenching with DMF provided the benzaldehyde intermediate **II** in 92% yield. Subsequent in situ dehydration of the oxime formed by reaction of the aldehyde with hydroxylamine provided the key fluorobenzonitrile **III** (54%, two steps). Condensation with hydrazine hydrate gave the bromo aminoindazole intermediate **IV** in 81% yield. Suzuki coupling with the phenyl boronic acid **V** afforded the final product **21**. Other examples were made in an analogous fashion to the route in Scheme 1 or by inverting the Suzuki reaction in step v. Specifically, reaction of the bromide **IV** with bis(pinacolato)diboron under palladium catalysis gave the dioxaborolane analog, which provided the additional final compounds after reaction with the appropriate aryl bromides.



Scheme 1. Reagents and conditions: (i) LDA, THF, −78 °C; (ii) hydroxylamine hydrochloride, EtOH, NaOAc, rt; (iii) Ac₂O, 140 °C; (iv) hydrazine hydrate, EtOH, 120 °C; (v) Boronic acid **V**, dppfCl₂Pd, Na₂CO₃; THF, MeCN, microwave, 120 °C.

In summary, we have shown how fragment-based hit identification coupled with crystallographically enabled structure-based drug design can provide potent inhibitors of JAK-2 and its clinically relevant V617F mutant. Of particular note is that after two iterations from fragment **1**, we were able to increase potency by greater than 500-fold to provide sulfonamide **13**, a 78-nM JAK-2 inhibitor. Our ongoing work in this area will be the subject of future publications.

Acknowledgments

Use of the Advanced Photon Source was supported by the U.S. Department of Energy, Office of Science, Office of Basic Energy Sciences, under Contract No. DE-AC02-06CH11357. Use of the SGX Collaborative Access Team (SGX-CAT) beamline facilities at Sector 31 of the Advanced Photon Source was provided by SGX Pharmaceuticals, Inc., who constructed and operates the facility.

References and notes

1. Leonard, W. J.; O'Shea, J. J. *Annu. Rev. Immunol.* **1998**, *16*, 293.
2. (a) Kisseleva, T.; Bhattacharya, S.; Braunstein, J.; Schindler, C. W. *Gene* **2002**, *285*, 1; (b) Levy, D. E.; Darnel, J. E. *Nat. Rev. Mol. Cell Biol.* **2002**, *3*, 651.
3. O'Shea, J. J.; Garndina, M.; Schreiber, R. D. *Cell* **2002**, *109*, S121.
4. Delhommeau, F.; Pisani, D. F.; James, C.; Casadevall, N.; Constantinescu, S.; Vainchenker, W. *Cell. Mol. Life Sci.* **2006**, *63*, 2939.
5. Levine, R. L.; Wadleigh, M.; Cools, J.; Ebert, B. L.; Wernig, G.; Huntly, B. J. P.; Boggon, T. J.; Wlodarska, I.; Clark, J. J.; Moore, S.; Adelsperger, J.; Koo, S.; Lee, J. C.; Gabriel, S.; Mercher, T.; D'Andrea, A.; Froehling, S.; Doehner, K.; Marynen, P.; Vandenberghe, P.; Mesa, R. A.; Tefferi, A.; Griffin, J. D.; Eck, M. J.; Sellers, W. R.; Meyerson, M.; Golub, T. R.; Lee, S. J.; Gilliland, D. G. *Cancer Cell* **2005**, *7*, 387.
6. Pardanani, A. *Leukemia* **2008**, *22*, 23.
7. Congreve, M.; Chessari, G.; Tisi, D.; Woodhead, A. J. *J. Med. Chem.* **2008**, *6*, 66. doi:10.1021/jm8000373.
8. Levinson, N. M.; Kuchment, O.; Shen, K.; Young, M. A.; Koldobskiy, M.; Karplus, M.; Cole, P. A.; Kuriyan, J. *PLoS Biol.* **2006**, *4*, 753.
9. Brameld, K. A.; Kuhn, B.; Reuter, D. C.; Stahl, M. J. *Chem. Inf. Mod.* **2008**, *48*, 1.